



Article

Transcriptome Analysis of 'Kyoho' Grapevine Leaves Identifies Heat Response Genes Involved in the Transcriptional Regulation of Photosynthesis and Abscisic Acid

Rongrong Guo ¹, Ling Lin ¹, Guiyuan Huang ¹, Xiaofang Shi ¹, Rongfu Wei ¹, Jiayu Han ¹, Sihong Zhou ¹ , Ying Zhang ¹, Taili Xie ¹, Xianjin Bai ^{2,*} and Xiongjun Cao ^{1,*}

¹ Grape and Wine Research Institute, Guangxi Academy of Agricultural Sciences, Nanning 530007, China

² Agricultural College, Guangxi Academy of Agricultural Sciences, Nanning 530007, China

* Correspondence: b5629@126.com (X.B.); cxj4310@126.com (X.C.); Tel.: +86-771-3245229 (X.C.)

Abstract: Grapevine is a popular cultivated fruit throughout the world and heat stress is one of the most serious threats to viticulture. However, transcriptional responses, such as molecular properties of photosynthesis and abscisic acid biosynthesis, metabolism and signal transduction pathway of grapevine to heat stress, are still poorly understood. In this study, RNA-seq was carried out for thermostabilized grapevine 'Kyoho' leaves. Results showed that 685 and 469 genes were commonly down-regulated and up-regulated at three sampling time-points. The light-dependent reactions of photosynthesis was significantly enriched in up-regulated DEGs at 1 hpt and down-regulated DEGs at R24 hpt. Heat stress impaired the photosynthetic capacity of grapevine leaves, and there was a significant positive relationship between photosynthesis and stomatal conductance at short-term post-heat stress treatment, but the inhibition of HS on P_n was non-stomata limitation for a longer period. Photosystem (PS)II was more sensitive to heat stress than PSI, and *PsbP*, as well as *Psb28*, played important roles in response to heat stress. The abscisic acid (ABA) content in heat-stress-treated Kyoho plants was higher than that in the control at 1 hpt, but less in heat-stress-treated plants at 4 and R24 hpt, which was regulated by numerous genes involved in the ABA biosynthesis and catabolism pathways. These results help to understand the influence of heat stress on photosynthesis and ABA biosynthesis, metabolism and signal transduction pathway.

Keywords: abscisic acid; grapevine; heat stress; photosynthesis; RNA-seq



Citation: Guo, R.; Lin, L.; Huang, G.; Shi, X.; Wei, R.; Han, J.; Zhou, S.; Zhang, Y.; Xie, T.; Bai, X.; et al. Transcriptome Analysis of 'Kyoho' Grapevine Leaves Identifies Heat Response Genes Involved in the Transcriptional Regulation of Photosynthesis and Abscisic Acid. *Agronomy* **2022**, *12*, 2591. <https://doi.org/10.3390/agronomy12102591>

Academic Editor: Min Gao

Received: 7 September 2022

Accepted: 18 October 2022

Published: 21 October 2022

Publisher's Note: MDPI stays neutral with regard to jurisdictional claims in published maps and institutional affiliations.



Copyright: © 2022 by the authors. Licensee MDPI, Basel, Switzerland. This article is an open access article distributed under the terms and conditions of the Creative Commons Attribution (CC BY) license (<https://creativecommons.org/licenses/by/4.0/>).

1. Introduction

Grapevine is one of the most economically important fruit crops in the world [1]. However, the production and quality of grapes are often affected by various environmental factors, including heat stress (HS) [2–5]. Studies indicated that when suffering from HS, photosynthetic, respiratory activities and berry quality were reduced, and the biosynthesis and accumulation of sugars, acids and anthocyanins in berries were also affected [6–8].

It has been reported that photosynthesis of grapevines was limited at temperatures above 35 °C and generally the restrictions were caused by stomatal limitation [9–14]. Several studies on grape leaves clearly showed that net photosynthetic rate (P_n) and stomatal conductance (G_s) sharply declined, while substomatal CO₂ concentration (C_i) abruptly rose at a temperature of over 40 °C [15,16]. During heat treatments, the reduction in photosynthesis of Semillon grapevine was attributed to 15–30% stomatal conductance [16,17], while Sepúlveda and Kliewer suggested stomatal limitation fully accounted for the reduction in photosynthesis [18].

Abscisic acid (ABA)-mediated responses are an important component of thermotolerance, and it was generally accepted that the ability to synthesize ABA under HS was the key factor attributed to the higher heat tolerance of a plant [19–21]. It has been noted that ABA is linked to HS signaling in different plant species, such as *Arabidopsis*, creeping bentgrass,

maize, and bromegrass [22–25]. In grape berry skin, the ABA catabolism/conjugation process and ABA biosynthetic pathway were also affected by water and heat stresses [26].

In previous works, many studies demonstrated that a series of heat shock transcription factors (HSFs) have a high transcript abundance in grapes under heat conditions, such as *VvHSEA2a* and *VpHSFB2b* [27,28]. Among 19 *Vv*HSFs, only *VSF01*, *VHSF05*, *VHSF15* and *VHSF18* showed different transcription levels in *V. vinifera* ‘Jingxiu’ (weak heat tolerance) and *V. davidii* ‘Tangwei’ (strong heat tolerance) under HS, indicating that these four *Vv*HSFs may be important factors underlying the thermotolerance difference between the two varieties [29].

Besides HSFs, some other genes have also been reported to participate in the tolerance of HS in grapes, such as heat shock proteins (HSPs) and members of the Bcl-2-associated athanogene family [30,31]. For example, enhanced levels of *HSP21* have been reported to be involved in alleviating HS and inducing decrease in *Pn* in salicylic acid (SA)-pretreated grapevine [15].

In recent years, with the advancement of biotechnology, more and more studies have investigated transcriptomic or proteomic changes in grapes post-HS. Liu et al., used Affymetrix Grape Genome oligonucleotide microarray to identify genes that were responsive to HS and/or to subsequent recovery in grape leaves, and found that the responsive genes belonged to a large number of important traits and biological pathways [5]. Proteins related to electron transport chains of photosynthesis, antioxidant enzymes, and HSPs may play key roles in enhancing grape adaption to and recovery capacity from HS in ‘Cabernet Sauvignon’ leaves [32]. In a recent study, high-throughput sequencing and the iTRAQ labeling technique was integrated to assess proteomic and transcriptomic changes in grape leaves under four different temperature regimes, and found alternative splicing, especially intron retention, was an important posttranscription regulatory event in response to high temperature [33]. RNA-seq has also been used to identify differentially expressed transcripts modulated by temperature in ripening grapevine fruits, and results showed that the tannin synthesis and degree of galloylation was impaired by high temperatures at the transcriptomic levels [34]. Admittedly, there are several more recent works using RNA-Seq profiles to investigate grapevine responses to heat [34–36], and many abiotic HS-induced genes and proteins have been identified [4], but our understanding of the molecular mechanisms involved in HS responses and thermotolerance in grape leaves is still insufficient. Thus, the dynamic transcriptomic changes in grape leaves in response to HS deserves a detailed investigation.

In the present study, we conducted transcriptomic analysis to elucidate the transcriptional changes at different time points post-HS and after recovery by RNA-seq, and the transcriptional levels of genes involved in photosynthesis and ABA biosynthesis, metabolism, and signaling transduction were analyzed further. The results from this study clarify the molecular mechanisms governing the heat-responsive processes involved in the transcriptional regulation of photosynthesis and ABA biosynthesis, metabolism, and signal transduction.

2. Materials and Methods

2.1. Plant Materials and Treatments

Stem cuttings of ‘Kyoho’ (*Vitis labrusca* × *Vitis vinifera* L.) were rooted in 2500 cm³ pots containing a mixture of 2 peat moss: 3 perlite (V/V) and grown for about 8 weeks in a controlled environment room under 25 °C (16 h light/8 h dark), 60–70% relative humidity. Water was irrigated once every two days, and 1/10 MS nutrient solution was supplied once a week, 300 mL per plant each time. Young grapevines with identical growth were acclimated for two days in an illuminating incubator (60–70% relative humidity, 26/20 °C day/night cycle and photosynthetic active radiation at 800 μmol m⁻²s⁻¹) and divided into two groups. On the following day (the first day of the experiment, Day 1), the first group was kept at 26/20 °C day/night in the illuminating incubator as the control. The second group was treated at 47 °C in another illuminating incubator from 10:00 a.m. to

14:00 p.m. The stressed grapevines were then subjected to 26 °C rapidly. All conditions were the same as the control until 14:00 p.m. on Day 2. Five randomly selected leaves from 5 plants of the treatment and control were sampled at 11:00 a.m. (1 h post heat treatment, 1 hpt) and 14:00 p.m. (4 h post heat treatment, 4 hpt) on Day 1 and 14:00 p.m. on Day 2 (24 h post recovery from heat treatment, R24 hpt) and immersed in liquid nitrogen and stored at −80 °C for transcriptomic analyses, quantitative real-time RT-PCR (qRT-PCR) analysis, and ABA content measurement. Chlorophyll fluorescence and gas exchange parameters were measured at 1, 4 and R24 hpt on the fifth leaf from the top of each plant. Five plants were used for the measurements and 2 data were obtained from each leaf. Three independently replicated experiments were executed.

2.2. RNA-Seq Analysis

Total RNA was extracted using the TRIZOL reagent (Takara, Dalian, China) according to the manufacturer's instructions. RNA quality analysis, library construction, and sequencing were performed by Biomarker Technologies (Beijing, China).

Raw data (raw reads) from fastq were firstly processed through in-house perl scripts. In this step, clean data (clean reads) were obtained by removing reads containing adapter, ploy-N and low quality reads. Then, clean reads were mapped to the reference grapevine genome (*Vitis_vinifera*.PN40024.v4.53.genome.fa) using HISAT2 [37,38]. Quantification of gene expression levels were estimated by fragments per kilobase of transcript per million mapped reads (FPKM) [39]. The formula is as follows:

$$\text{FPKM} = \frac{\text{cDNA Fragments}}{\text{Mapped Fragments (Millions)} \times \text{Transcript Length (kb)}} \quad (1)$$

2.3. Gene Function Annotations and Classifications

Gene function was annotated based on the following databases: NCBI non-redundant protein sequence database (Nr), NCBI non-redundant nucleotide sequences (Nt), Protein family (Pfam), Swiss-Prot, Cluster of Orthologous Groups of proteins (COG), the database of Clusters of Protein homology (KOG), Kyoto Encyclopedia of Genes and Genomes Ortholog database (KO) and Gene Ontology (GO).

2.4. Identification of Differentially Expressed Genes (DEGs)

Differentially expressed genes (DEGs) between the samples were identified by 'DESeq2' [40]. The resulting *p* values were adjusted using the Benjamini–Hochberg approach for controlling the false discovery rate (FDR). Genes with fold change ≥ 2 , FDR ≤ 0.01 , and an adjusted *p* value < 0.01 found by DESeq2 were regarded as DEGs.

GO enrichment analysis of the DEGs was implemented by the Goseq R packages based Wallenius non-central hyper-geometric distribution [41]. KOBAS software was used to test the statistical enrichment of DEGs in KEGG pathways [42].

2.5. Validation of RNA-Seq by Quantitative Real-Time RT-PCR

Total RNA extraction was the same as that used for RNS-seq analysis described above. First-strand cDNA was synthesized using the Superscript II reverse transcriptase (Invitrogen) with an oligo(dT)15 primer according to the manufacturer's instructions (Tiangen Biotech, Beijing, China). Twelve DEGs were chosen to confirm that they involve in responding to HS using quantitative real-time RT-PCR method. All the genes were normalized with *VvEF1- α* and *VvActin*. The selected DEGs and their corresponding primer sequences are provided in Table S1. qRT-PCR was performed using the LightCycler® 480 SYBR Green I Master (Roche) with 10 pmol of each primer, and the reactions were run on a LightCycler® 480 (Roche). All reactions were performed in triplicate, and the normalized relative expression levels were calculated with the $2^{-\Delta\Delta C_t}$ method [43]. Pearson correlation coefficients (*p*-value < 0.01) were calculated to assess the correlations between the different expression patterns obtained by qRT-PCR and RNA-seq.

2.6. Analysis of Photosynthetic Gas Exchange

Photosynthetic gas exchange was analyzed with an open-path infrared gas analyser system (CIRAS-3, PP system, Amesbury, USA) which can assess photosynthesis by means of photosynthetic photon flux density (PPFD), leaf temperature and CO₂ concentration in the cuvette. *P_n*, *G_s*, *C_i* and transpiration rate (*T_r*) were determined at a concentration of ambient CO₂ (400 ppm) and a PPFD of 1200 μmol m⁻² s⁻¹.

2.7. Measurement of Chlorophyll Fluorescence

Chlorophyll fluorescence was measured using a Handy Plant Efficiency Analyser (Hansatech Instrument, King's Lynn, UK) on the fifth leaf from the top using a previously standardized protocol [44]. The leaves were clipped in the middle using leaf dark clips (Hansatech Instrument) for 30 min at 26 °C (control) or 47 °C (HS) before measurement. The maximum quantum efficiency of PSII photochemistry (*F_v/F_m*) was measured on the adaxial leaf surface immediately after the dark adaptation using a PPFD of 3000 μmol m⁻² s⁻¹ as saturating flash for the duration of 1 s. The following PSII behaviour parameters were calculated per excited leaf cross-section (CSm): *ABS/CSm* (absorption flux per CSm approximated), *TRO/CSm* (trapped energy flux per CSm), *RC/CSm* (percentage of active/inactive reaction centers per CSm), *ETo/CSm* (electron transport flux per CSm), *DIO/CSm* (dissipated energy flux per CSm).

2.8. Measurement of Endogenous ABA Content

The ABA content was measured using the method of enzyme-linked immunosorbent assay as described previously [45].

2.9. Statistical Analysis

Significant differences were determined when *p* < 0.05 according to independent *t*-tests. Heatmap was performed with MetaboAnalyst 5.0, and statistical analysis was performed with SPSS (SPSS Inc., Chicago, IL, USA) for Windows, version 26.0.

3. Results

3.1. Illumina Sequencing

Eighteen cDNA libraries were generated with mRNA from the six sample groups: group1 (heat treatment exposed at 47 °C for 1 h, H1), group2 (heat treatment exposed at 47 °C for 4 h, H4), group3 (24 h post recovery from heat treatment exposed at 47 °C for 4 h, HR24), group4, 5, and 6 (control at 26 °C for 1 h, 4 h and 28 h, respectively, namely as C1, C4, and CR24) for the full expanded leaf. These cDNA libraries were then subjected to Illumina HiSeq 2000 sequencing. After removing reads of low quality, adapter sequences, or reads with more than 5% ambiguous nucleotides, a total of 501,871,839 clean reads were produced consisting of 146,372,337,142 nucleotides (146.37 Gb), with an average GC content of 45.7%. Reads mapping to the genome sequence ranged from 85.26% to 89.31% of the reads (Table S2). To better understand the distribution of the samples according to the six groups, the principal component analysis (PCA) for the 18 samples was carried out based on the gene expression level. Results showed the first two principal components accounted for 91.9% of the variation, the three samples of each group clustered together, and the distances among three groups of HS treatment were much greater than that of the control (Figure S1A). To further investigate the robustness of the RNA-Seq dataset, the correlation coefficients of the transcriptome profiles among the 18 samples were calculated and were found to reach 0.97 between three biological replicates of each group (Figure S1B).

3.2. DEGs among the HS Treatment and Control in Grape

A total of 11,097 differentially expressed transcripts between HS treatment and control were obtained. Among these DEGs, 2631 were down-regulated and 1889 were up-regulated at 1 h post HS treatment (hpt), 3379 were down-regulated and 2817 were up-regulated at 4 hpt, while 2943 were repressed and 1952 were induced at 24 h after recovery from 4 h

of HS treatment (R24 hpt) compared to their corresponding control (Figure 1A). A total of 469 genes were commonly up-regulated at the three sampling time-points by HS treatment (Figure 1B), and the top five enriched GO terms of these 469 DEGs in the 'biological process' category were 'response to heat', 'response to hydrogen peroxide', 'response to reactive oxygen species', 'protein oligomerization', and 'protein folding'. In the 'cellular component' category, the top five enriched GO terms of the commonly up-regulated DEGs were 'Cajal body', 'telomerase holoenzyme complex', 'nucleus', 'mitochondrial intermembrane space' and 'mitochondrial respiratory chain complex I'. In the 'molecular function' category, the top five enriched GO terms of the commonly up-regulated DEGs were 'unfolded protein binding', 'protein self-association', 'protein binding involved in protein folding', 'heat shock protein binding', and 'misfolded protein binding' (Figure 1C). A total of 685 genes were commonly down-regulated at the three sampling time-points by HS treatment (Figure 1D). The top five enriched GO terms of the commonly down-regulated 685 genes in 'biological process' category were 'hormone-mediated signaling pathway', 'pectin catabolic process', 'defense response', 'chitin catabolic process', and 'brassinosteroid metabolic process'. In the 'cellular component' category, the top five enriched GO terms of the commonly down-regulated DEGs were 'integral component of membrane', 'extracellular region', 'plasma membrane', 'cell wall', and 'plant-type cell wall'. In the 'molecular function' category, the top five enriched GO terms of the commonly down-regulated DEGs were 'protein kinase activity', 'protein serine/threonine kinase activity', 'ATP binding', 'transferase activity, transferring acyl groups other than amino-acyl groups', and 'aspartic-type endopeptidase activity' (Figure 1E).

To validate the transcriptional pattern identified by RNA-seq, the expression of 12 DEGs was analyzed using qRT-PCR. The correlation coefficients of 0.731 indicated the credibility of the results of the RNA-Seq-based gene expression (Figure S2).

3.3. KEGG Pathway Enrichment Analysis of DEGs

KEGG Orthology-Based Annotation System (<http://kobas.cbi.pku.edu.cn/home.do>, accessed on 10 June 2022) were used to test the statistical enrichment pathways for up- or down-regulated DEGs between HS treatment and control [42]. According to the KEGG pathway analysis, both 'Protein processing in endoplasmic reticulum' and 'Zeatin biosynthesis' were contained in the top 10 enriched pathways of up-regulated DEGs at the three sampling time-points (Figure 2A,C,E), while 'Plant-pathogen interaction', 'Plant hormone signal transduction' and 'MAPK signaling pathway-plant' were contained in the top 10 enriched pathways of down-regulated DEGs at the three sampling time-points (Figure 2B,D,F). It should be noted that 'Photosynthesis' was significantly enriched in up-regulated DEGs at 1 hpt and down-regulated DEGs at R24 hpt (Figure 2A,F). 'Ribosome', 'Porphyrin and chlorophyll metabolism', 'RNA degradation', and 'Arachidonic acid metabolism' were enriched in up-regulated DEGs at 1 and 4 hpt (Figure 2A,C), while 'Circadian rhythm-plant', 'Spliceosome', and 'Glycosphingolipid biosynthesis—lacto and neolacto series' were enriched in down-regulated DEGs at 1 and 4 hpt (Figure 2B,D). 'Carotenoid biosynthesis' and 'Cysteine and methionine metabolism' were enriched in up-regulated DEGs at 4 and R24 hpt (Figure 2C,E), while 'Fatty acid elongation' and 'other glycan degradation' were enriched in down-regulated DEGs at 4 and R24 hpt (Figure 2D,F).

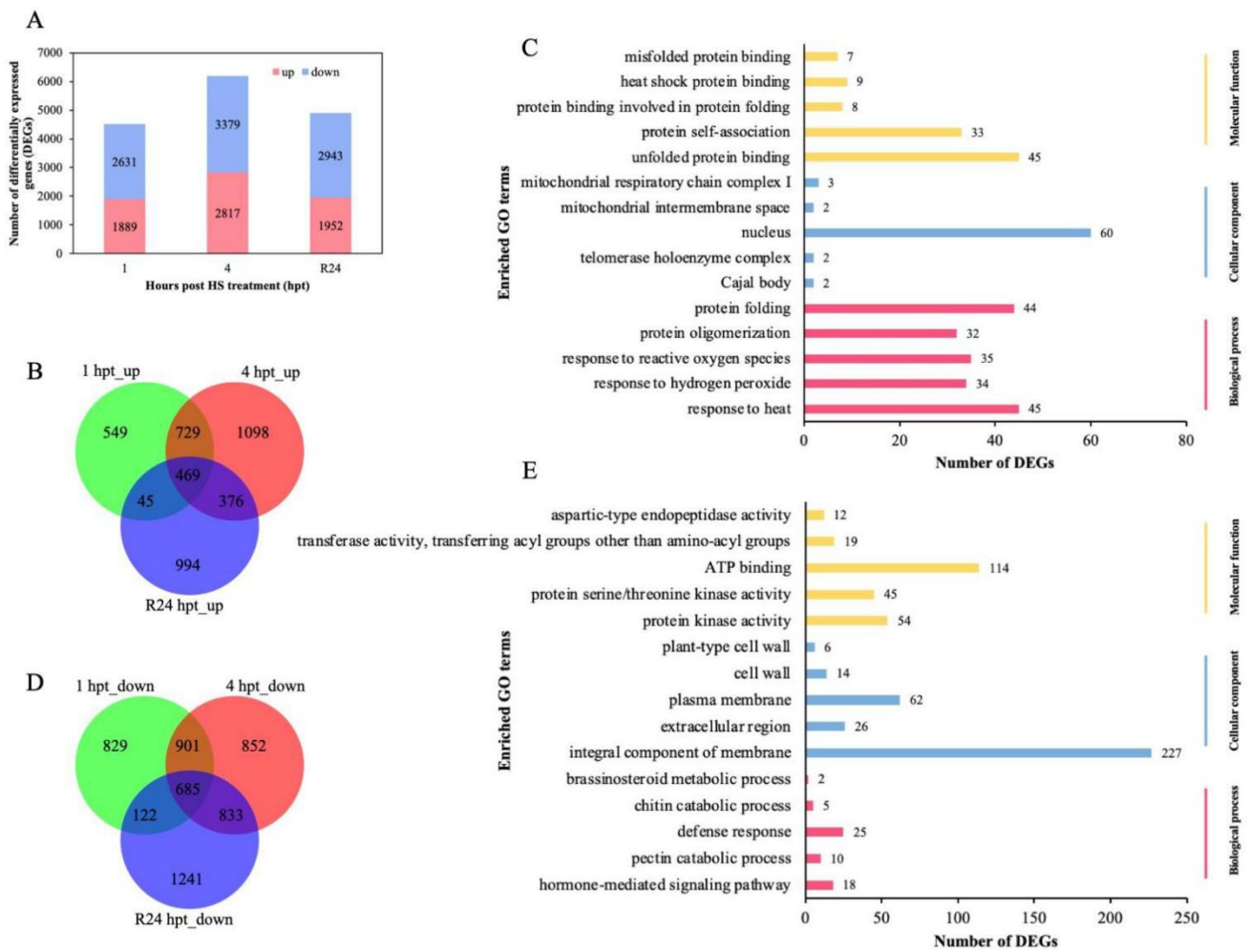


Figure 1. Comparison of gene expression at 1, 4 h post-HS treatment (hpt) and 24 h after recovery from 4 h of HS treatment (R24 hpt) between HS-treated grapevines and control. (A) Number of DEGs (p -value ≤ 0.05 and fold-change ≥ 2) between HS-treated grapevines and control at three sampling time points. (B) Venn diagram showing the relationship among up-regulated DEGs at 1, 4, and R24 hpt. (C) The top five enriched GO terms of commonly up-regulated DEGs at the three sampling time-points in the ‘biological process’, ‘cellular component’ and ‘molecular function’ categories. (D) Venn diagram showing the relationship between down-regulated DEGs at 1, 4, and R24 hpt. (E) The top five enriched GO terms of commonly down-regulated DEGs at the three sampling time-points in the ‘biological process’, ‘cellular component’ and ‘molecular function’ categories.

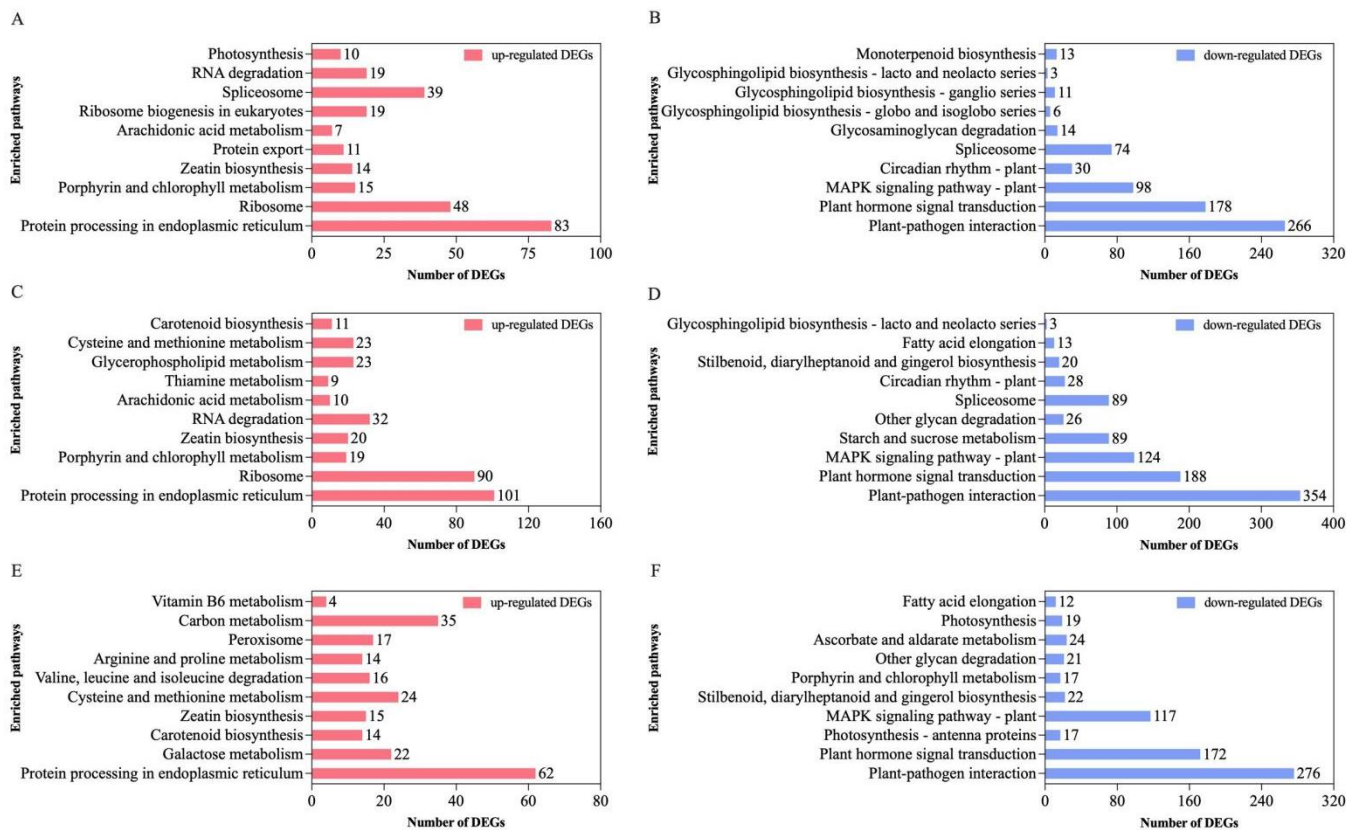


Figure 2. The top 10 enriched pathways of DEGs between HS-treated grapevines and control. (A) The top 10 enriched pathways of up-regulated DEGs at 1 hpt. (B) The top 10 enriched pathways of down-regulated DEGs at 1 hpt. (C) The top 10 enriched pathways of up-regulated DEGs at 4 hpt. (D) The top 10 enriched pathways of down-regulated DEGs at 4 hpt. (E) The top 10 enriched pathways of up-regulated DEGs at R24 hpt. (F) The top 10 enriched pathways of down-regulated DEGs at R24 hpt.

3.4. Effect of HS Treatment on Gas Exchange

To explore the effect of HS treatment on photosynthesis, P_n , G_s , C_i and Tr were measured at 1, 4 and R24 hpt. It was showed that P_n in leaves of HS-treated grapevines was decreased by 67.97% at 1 hpt, when compared with that of the control, and it was decreased by 102.93% at 4 hpt. After recovery from HS, the P_n was raised, but was even lower than that of the control at R24 hpt (Figure 3A). The C_i in leaves of HS-treated plants was increased to 1.25- and 1.1-fold when compared with control at 4 and R24 hpt, respectively (Figure 3B). It was noteworthy that G_s and Tr in leaves of HS-treated grapevines was decreased by 67.48% and 58.92% at 1 hpt, respectively, but the two parameters were increased by 2.18- and 1.33-fold at 4 hpt, respectively. After recovery from HS, G_s and Tr were decreased, but G_s in leaves of HS-treated grapevines was still higher than that of the control (Figure 3C,D).

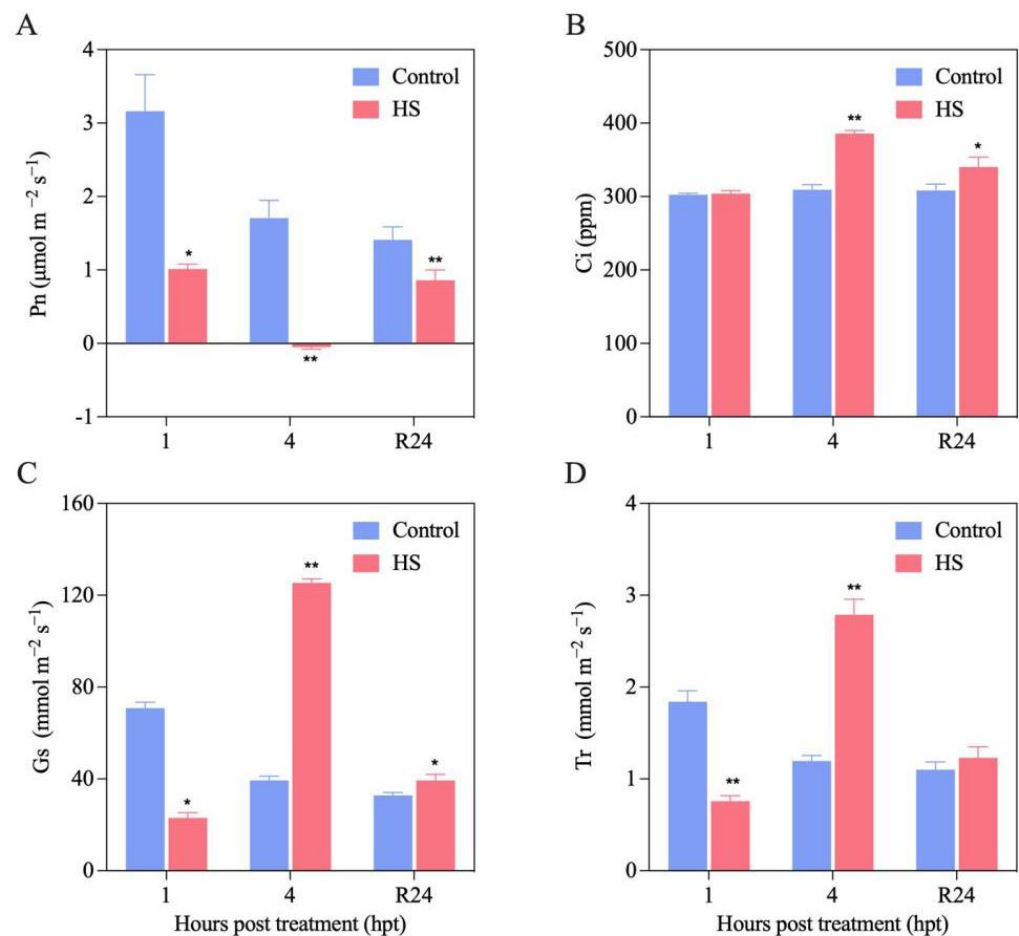


Figure 3. Effect of HS treatment on gas exchange parameters. (A) net photosynthetic rate (Pn), (B) intercellular CO₂ concentration (Ci), (C) stomatal conductance (Gs), (D) transpiration rate (Tr). Gas exchange parameters were measured on the fifth leaf from the top of each plant at a CO₂ concentration of 400 $\mu\text{mol mol}^{-1}$ and a PPFD of 1200 $\mu\text{mol m}^{-2} \text{s}^{-1}$. Asterisks indicate statistical significance (* 0.01 < p < 0.05, ** p < 0.01, Student's t -test) of differences between the HS treatment and control at three sampling time-points. Data represent mean values \pm SD from three independent experiments.

3.5. Effect of HS Treatment on Donor Side, Reaction Center and Acceptor Side of PSII

In the present study, Fv/Fm was decreased significantly at 1 and 4 hpt, but not significantly at R24 hpt (Figure 4A). Besides the Fv/Fm, on a per-unit excited leaf cross-section (CSm), ABS/CSm was also decreased significantly at 1 and 4 hpt, and to a minimum at 4 hpt (Figure 4B). ETo/CSm, TRo/CSm, and RC/CSm was decreased significantly at all of the three sampling time-points, and to a minimum at 4 hpt (Figure 4C–E), while DIo/CSm was increased significantly at 4 and R24 hpt (Figure 4F).

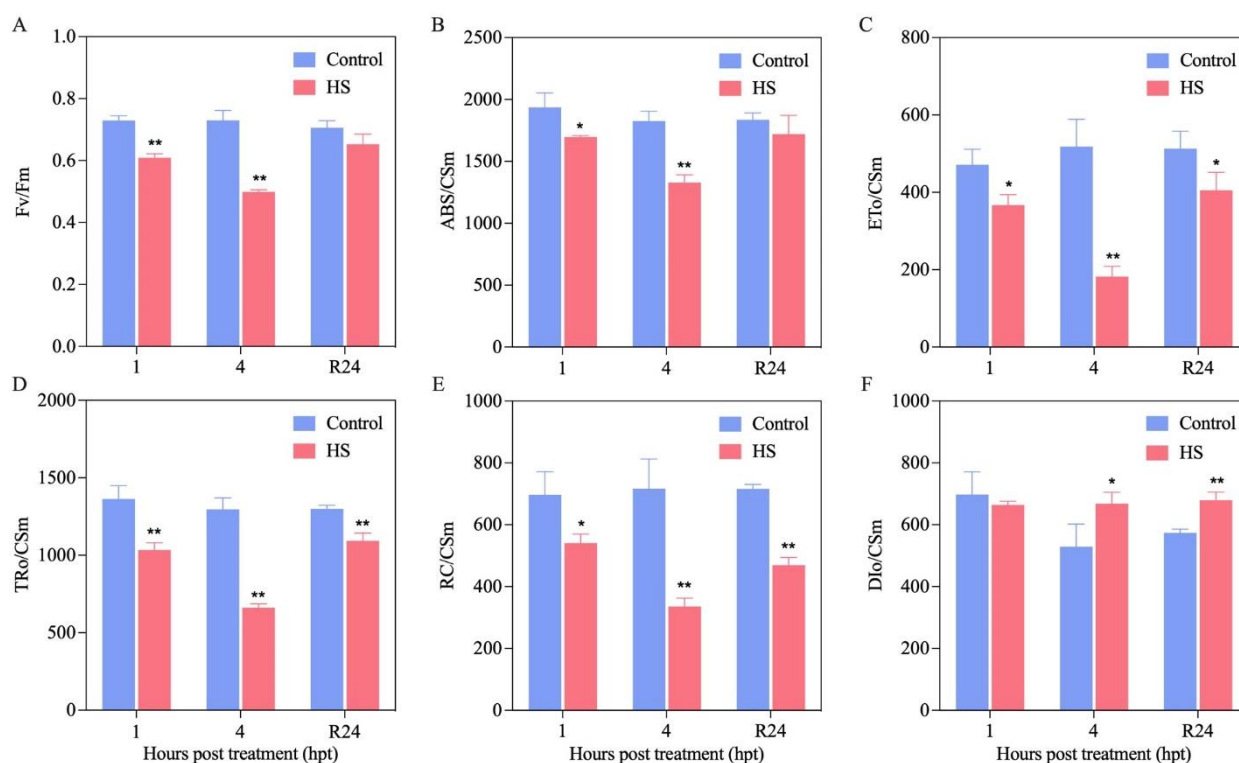


Figure 4. Effect of HS treatment on chlorophyll fluorescence. (A) Fv/Fm (the maximum quantum efficiency of PSII photochemistry), (B) ABS/CSm (absorption flux per CSm approximated), (C) ETo/CSm (electron transport flux per CSm), (D) TRo/CSm (trapped energy flux per CSm), (E) RC/CSm (percentage of active/inactive reaction centers per CSm), (F) Dlo/CSm (dissipated energy flux per CSm). Asterisks indicate statistical significance (* $0.01 < p < 0.05$, ** $p < 0.01$, Student's *t*-test) of differences between the HS treatment and control at three sampling time-points. Data represent mean values \pm SD from three independent experiments.

3.6. Effect of HS Treatment on Expression of Photosynthesis-Related Genes

To explore the differences in gene expression profiles at different time points post-HS treatment as well as recovery from HS, a KEGG (<http://www.genome.jp/kegg/>, accessed on 10 June 2022) pathway enrichment analysis revealed that 34 DEGs were involved in photosynthesis. These DEGs covered all sections of the pathway, including PSII, photosynthetic electron transport, cytochrome b6/f complex, F-type ATPase, and PSI.

In PSII, the expression of *PsbA* (*Vitvi13g00384*) was up-regulated at 1 and R24 hpt, *PsbP* (*Vitvi13g00254*) was up-regulated at 1 and 4 hpt, while another *PsbP* gene (*Vitvi04g01013*) and *Psb28* (*Vitvi07g00690*) were up-regulated at 1 hpt. *PsbQ* (*Vitvi10g02212*) was down-regulated at 4 and R24 hpt. Other DEGs in PSII, including *PsbO* (*Vitvi18g00894*), *PsbW* (*Vitvi07g00035* and *Vitvi14g00489*), and *PsbY* (*Vitvi01g00589*) were down-regulated at R24 hpt (Figure 5, Table S3).

In photosynthesis electron transport, the expression of *PetE* (*Vitvi18g00158*) and *PetH* (*Vitvi18g01130*) was decreased at R24 hpt, while *PetF* (*Vitvi05g00505*) was up-regulated at 4 hpt. In cytochrome b6/f complex, the expression of *PetA* (*Vitvi_newGene_3356*, and *Vitvi00g04187*) was up-regulated at 1 hpt, and kept normal at 4 and R24 hpt, while *PetB* (*Vitvi00g04882*) was down-regulated at 4 hpt. The expression of *PetC1* (*Vitvi19g00308*) was increased at 1 and 4 hpt, while *PetC2* (*Vitvi03g01127*) was only significantly induced at 4 hpt. In F-type ATPase, the subunits *Beta* (*Vitvi14g02960*) and *gamma* (*Vitvi19g00504*) was down-regulated at 4 hpt and 1 hpt, respectively. The ATPase subunit *c* (*Vitvi10g04459*) was down-regulated at 4 and R24 hpt, while the ATPase subunit *b* (*Vitvi01g04467*) was up-regulated at R24 hpt (Figure 5, Table S3).

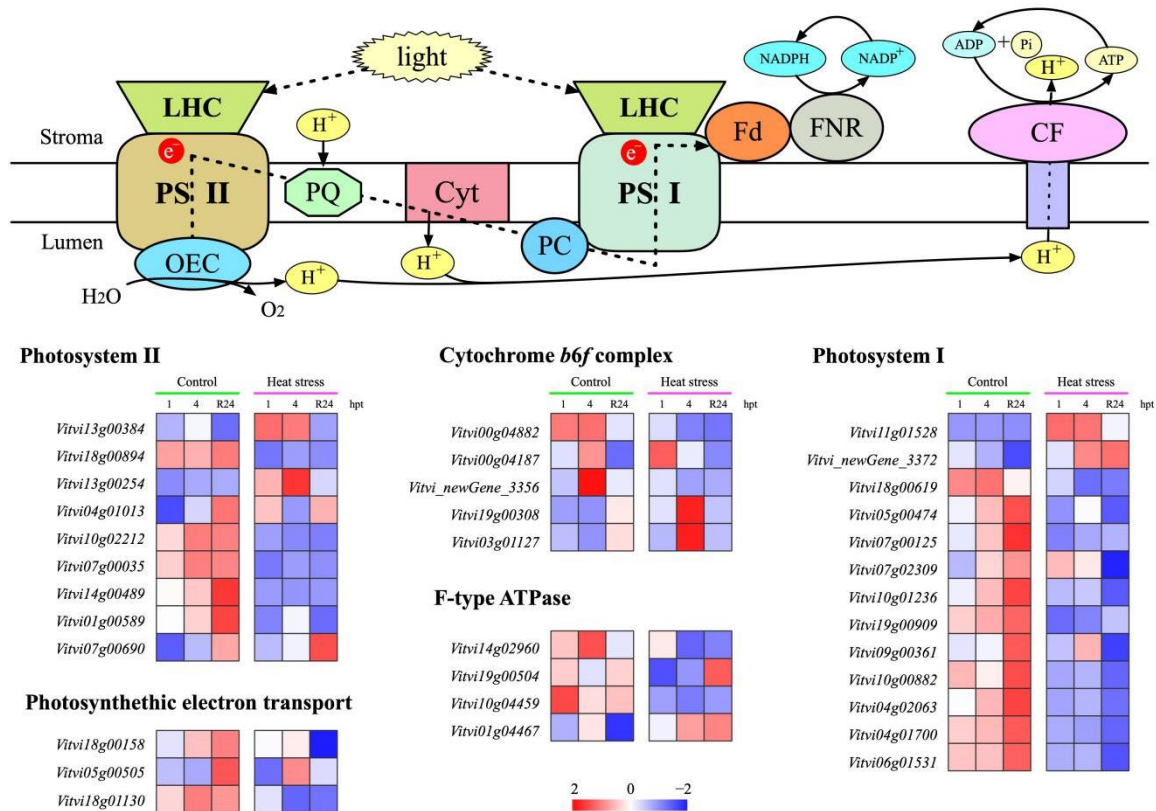


Figure 5. Transcriptomic profiles of DEGs involved in photosynthesis pathway following HS treatment and subsequent recovery. Different shades of red and blue express the average FPKM value (log₂ transformed) of the gene in each sample, as illustrated in the legend.

In PSI, the expression of *PsaA* (*Vitvi11g01528*) was up-regulated at all three sampling time-points. One of the *PsaB* genes (*Vitvi18g00619*) was down-regulated at 4 hpt and R24 hpt, while another *PsaB* gene (*Vitvi_newGene_3372*) was up-regulated at the two sampling time-points. The expression of *PsaE* (*Vitvi07g02309*) was up-regulated at 1 hpt, and it was down-regulated at R24 hpt. Other DEGs in PSI, including *PsaD* (*Vitvi05g00474* and *Vitvi07g00125*), *PsaF* (*Vitvi10g01236*), *PsaG* (*Vitvi19g00909*), *PsaH* (*Vitvi09g00361*), *PsaK* (*Vitvi10g00882*), *PsaL* (*Vitvi04g02063*), *PsaN* (*Vitvi04g01700*) and *PsaO* (*Vitvi06g01531*) were down-regulated at R24 hpt (Figure 5, Table S3).

3.7. Effect of HS Treatment on Expression of ABA Biosynthesis, Catabolism and Signal Transduction-Related Genes

In the present study, we measured the ABA content in grape leaves post-HS treatment, and results showed that the ABA content in HS-treated plants was more than that in control at 1 hpt, but it was less in HS-treated plants at 4 and R24 hpt (Figure S3). To explore the differences in gene expression patterns at different time points post-HS treatment as well as recovery from HS, a KEGG pathway enrichment analysis revealed that 42 genes encoding 14 enzymes or proteins were involved in ABA biosynthesis, metabolism and signal transduction pathway (Figure 6, Table S4).

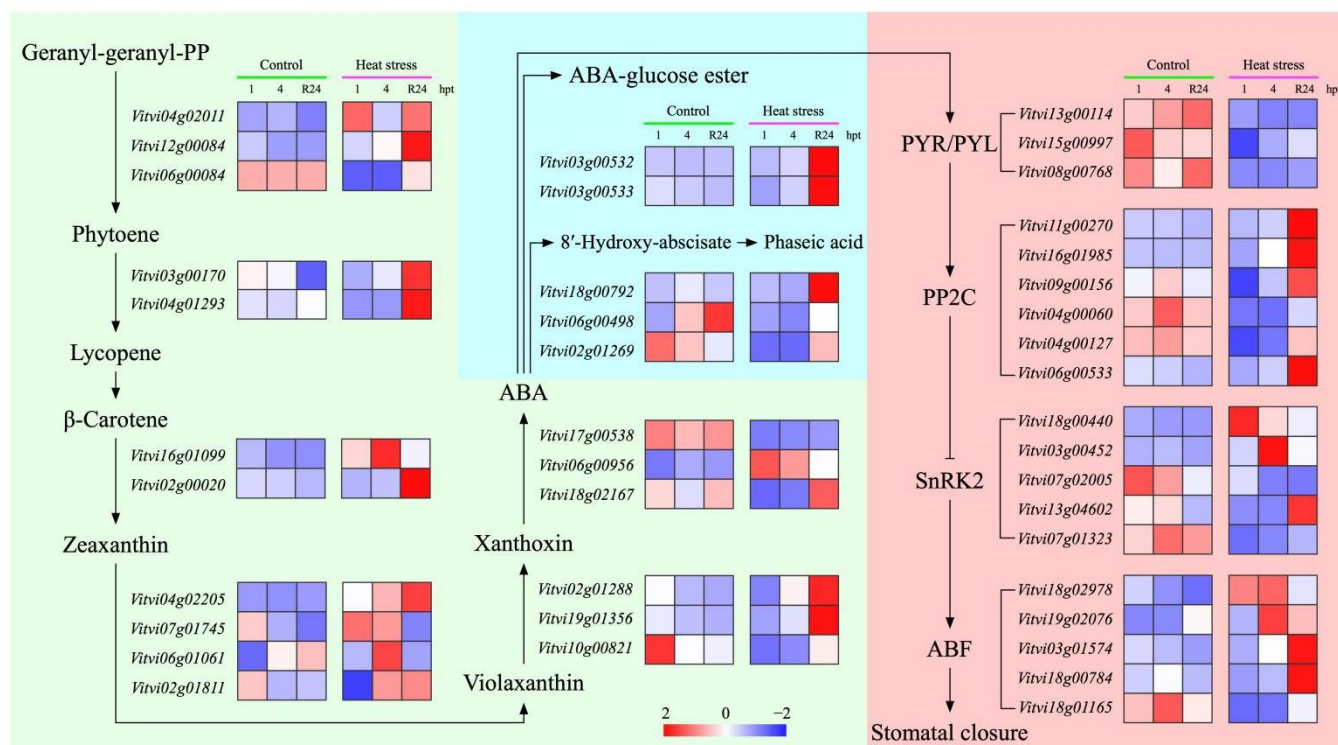


Figure 6. Transcriptomic profiles of DEGs involved in the ABA biosynthesis, metabolism, and signal transduction pathways following HS treatment and subsequent recovery. Different shades of red and blue express the average FPKM value (log₂ transformed) of the gene in each sample, as illustrated in the legend.

In the ABA biosynthesis pathway, most DEGs were up-regulated or kept normal at the three sampling time-points, except for one *phytoene synthase 2 (PSY2)* gene (*Vitvi06g00084*) and *9-cis-epoxycarotenoid dioxygenase 2 (NCED2)*, (*Vitvi10g00821*), which were down-regulated at 1 and 4 hpt, as well as *NCED 4* (*Vitvi02g01288*) and *NCED1* (*Vitvi19g01356*); both were down-regulated at 1 hpt, and up-regulated at 4 and R24 hpt, and *ABA2* (*Vitvi17g00538*), whose expression was decreased at the three sampling time-points. The expression of 1 *AAO3* (*Vitvi18g02167*) was decreased at 1 hpt, and remained normal at 4 and R24 hpt (Figure 6, Table S4).

In the ABA catabolism process, *ABA 8'-hydroxylase (ABA8ox)*, EC: 1.14.13.93) and *ABA glucosyltransferase (ABA-GT)*, EC: 2.4.1.263) are the major enzymes for phaseic acid (PA) and ABA glucosyl-ester (ABA-GE), respectively [46]. Compared with that in control, the expression of *ABA-GT* (*Vitvi03g00533*) was decreased at 1 hpt, and increased at R24 hpt, another *ABA-GT* gene (*Vitvi03g00532*) was up-regulated at R24 hpt. Three genes annotated as *ABA8ox* were identified, and their expression levels were variable. Among them, *ABA8ox1* (*Vitvi02g01269*) was down-regulated at 1 and 4 hpt, *ABA8ox2* (*Vitvi06g00498*) was down-regulated at 4 and R24 hpt, while the expression of *ABA8ox4* (*Vitvi18g00792*) was induced at R24 hpt (Figure 6, Table S4).

In ABA signal transduction pathway, the expression of ABA receptors *PYRs/PYLs* were decreased at one or more sampling time-points. *Type 2C serine threonine protein phosphatase 2C 72 (PP2C 72)*, (*Vitvi04g00060*) and *PP2C53* (*Vitvi04g00127*) were down-regulated at 1 and 4 hpt, *PP2C24* (*Vitvi06g00533*) was down-regulated at 1 hpt and up-regulated at R24 hpt, *PP2C 16* (*Vitvi09g00156*) was down-regulated at 1 hpt, and *PP2C 8* (*Vitvi16g01985*) was up-regulated at 4 and R24 hpt, while *PP2C68* (*Vitvi11g00270*) was up-regulated at R24 hpt. Five DEGs annotated as *SNF1-related type 2 protein kinases (SnRK2)* were identified in this study. Among them, *SAPK2* (*Vitvi18g00440*) and *SAPK10* (*Vitvi03g00452*) were up-regulated at 1 and 4 hpt, and the later was also up-regulated at R24 hpt. *SAPK3* (*Vitvi13g04602*) was down-regulated at 4 hpt and up-regulated at R24 hpt. Both *SnRK2A* (*Vitvi07g02005*) and

SnRK2I (*Vitvi07g01323*) were down-regulated at 4 and R24 hpt. Five DEGs were annotated as *ABA responsive element binding factor* (*ABF*) in this study. Among them, two DEGs named as *G-box-binding factor 4* (*Vitvi18g02978* and *Vitvi19g02076*) were up-regulated at 4 hpt and the former was up-regulated at 1 hpt. Two DEGs named as *ABI5-5* (*Vitvi03g01574* and *Vitvi18g00784*) were up-regulated at R24 hpt. One DEG named as *FD* (*Vitvi18g01165*) was down-regulated at 1 and 4 hpt (Figure 6, Table S4).

3.8. Effect of HS Treatment on Expression of HSPs and HSFs

In this study, 68 DEGs of the *HSPs* family were detected in the HS-treated grapevine transcriptome. Among these DEGs, 55 were up-regulated at all three sampling time-points, including 1 *HSP101*, 1 *HSP70-HSP90* organizing protein, 3 *HSP90*, 9 *HSP70*, and 41 *HSP20*, while *HSP90-5* (*Vitvi01g01311*), 2 *HSP80* (*Vitvi10g00217* and *Vitvi19g02080*), and 5 *HSP70* (*Vitvi06g01693*, *Vitvi07g01524*, *Vitvi09g00876*, *Vitvi13g00300*, and *Vitvi17g00287*) were up-regulated at 1 and 4 hpt, and remained normal at R24 hpt. One *HSP70* (*Vitvi04g01014*) and 1 *HSP20* (*Vitvi18g01510*) were up-regulated at 4 hpt, and kept normal at 1 and R24 hpt. One *HSP20* (*Vitvi17g01454*) was down-regulated at 4 hpt, 1 *HSP20* (*Vitvi10g02289*) was down-regulated at R24 hpt, and 1 *HSP20* (*Vitvi10g00134*) was down-regulated at 4 and R24 hpt (Figure 7A, Table S5).

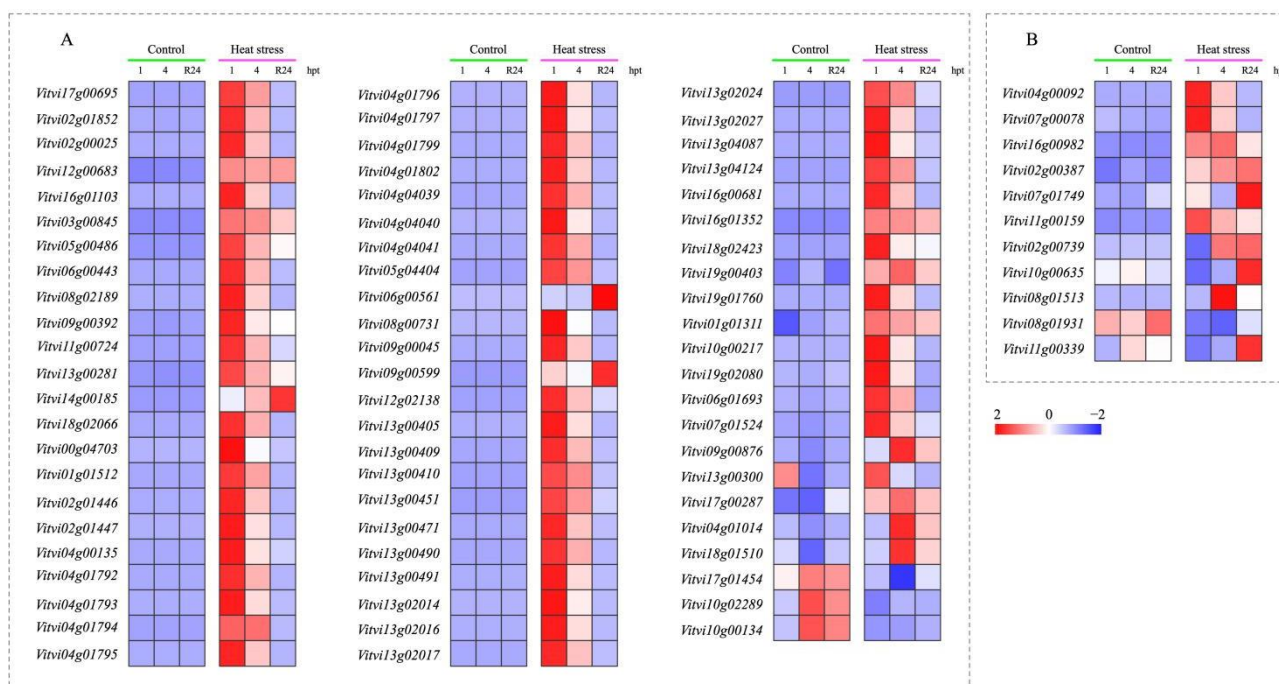


Figure 7. Transcriptomic profiles of DEGs contained in the HSP (A) and HSF (B) families following HS treatment and subsequent recovery. Different shades of red and blue express the average FPKM value (log2 transformed) of the gene in each sample, as illustrated in the legend.

Among our data, *HSF30* (*Vitvi04g00092*), *HSEA6b* (*Vitvi07g00078*), *HSFB2a* (*Vitvi16g00982*), and *HSFB2b* (*Vitvi02g00387*) were significantly up-regulated at all of the three sampling time-points, *HSF24* (*Vitvi07g01749*) and *HSEA7a* (*Vitvi11g00159*) were up-regulated at 1 and R24 hpt, *HSF8* (*Vitvi02g00739*) and *HSEA4a* (*Vitvi10g00635*) were up-regulated at 4 hpt and R24 hpt, respectively, and *HSEA2e* (*Vitvi08g01513*) was up-regulated at 4 and R24 hpt. *HSFB3* (*Vitvi08g01931*) was down-regulated throughout all time points, and *HSFC1* (*Vitvi11g00339*) was down-regulated at 1 and 4 hpt, but up-regulated at R24 hpt (Figure 7B, Table S6).

4. Discussion

Since the response of plants to HS is an intricate physiological process, there are various pathways intertwined closely to regulate this mechanism. These mechanisms include physiological adaptations, such as photosynthesis and activation of signaling pathways, and gene regulatory networks inducing the expression of HSFs and HSPs governing HS response and acquisition of thermotolerance [4,5,47]. Therefore, it is not strange that thousands of genes were successfully detected as responsive to HS treatment. In the present study, we set up a control at each sampling time point to eliminate the influence of time change in a day.

Finally, compared with the control at each time point, 4520, 6196, and 4895 genes were identified to be regulated by HS at 1, 4 and R24 hpt, respectively. Among them, 685 and 469 genes were commonly down-regulated and up-regulated at the three sampling time-points, respectively. A few studies also reveal the molecular-level changes of grapes in response to HS. Using microarray analysis, Liu et al., showed that only 12 genes were usually up-regulated due to HS and recovery, and only 73 genes were generally down-regulated [5]. Compared with the results of our experiment, the much smaller number of differentially expressed genes may be due to the different experimental technique. Additionally, using the transcriptome technique, Ju et al., detected 1727 up-regulated genes and 1231 down-regulated genes in response to HS in Cabernet Sauvignon grapevine cuttings [48], and Liu et al., identified 1728 up-regulated and 1232 down-regulated genes in heat-treated Cabernet Sauvignon grapevine compared with control [49]. The difference between these two results and our study may be due to the difference of heat treatment methods and may also be related to the ploidy of varieties. The Cabernet Sauvignon grapevine is diploid, while the variety used in this study (Kyoho) is tetraploid. Previous studies showed that the ploidy levels can affect the gene expression and the classical RNA-Seq normalization approach may not be appropriate for the comparison of samples with different ploidy levels [50,51]. As polyploids have more than two basic sets of chromosomes, the number of each allele on the chromosome also increases, which may lead to gene higher expression and more obvious growth advantages than diploid plants [51]. Polyploidy breeding may also be a rapid strategy for adaptation to stress conditions. Compared with the previous experiment, the tetraploid variety (Kyoho) used in this experiment has a stronger response to high temperature stress at the gene expression level. This seems to give a molecular biological explanation for the heat resistance of thermostabilized polyploid grapes.

The responsive genes identified in this study were classified under a large number of GO terms and KEGG pathways. Of particular interest, genes involved in photosynthesis and ABA biosynthesis, metabolism, and signal transduction, as well as HSFs and HSPs were further analyzed. Gas exchange parameters, chlorophyll fluorescence and ABA content in HS treated grapevine leaves were measured.

4.1. Photosynthesis Was Inhibited by HS Treatment

Previous studies have reported that photosynthesis was the most critical process in plants that was directly or indirectly affected by temperature, and was very sensitive even in short-term temperature fluctuations [4,14,33,52]. Extremely high temperatures (above 40 °C) cause damage to photosynthetic apparatus and have a severe impact on photosynthesis [4]. In our study, P_n in leaves of HS-treated grape plants was decreased at all of the three sampling time-points, and even to a negative value at 4 hpt, but C_i was much higher under HS treatment than control at 4 and R24 hpt (Figure 3A,B), suggesting the photosynthesis system was deeply inhibited by HS treatment and the decreased P_n was not caused by the shortage of carbon dioxide supply [14,53], although tetraploid Kyoho may have higher stress tolerance [54]. It is worth noting that in HS-treated Kyoho grapevine, G_s was decreased at 1 hpt, but increased at 4 and R24 hpt (Figure 3C), but in Semillon grapevine, both stomatal conductance and photosynthesis were significantly reduced immediately after the heat treatment [17]. When refer to the relationship between photosynthesis and stomatal conductance, there were two opposite viewpoints, Sepúlveda and Kliwer and Matsui et al.,

suggested that stomatal limitation fully accounted for the change in photosynthesis [18,55], while Godde and Bormann held the view that stomatal conductance appeared to play only a minor role in the temperature limitation of photosynthesis [56]. From the analysis of gas exchange parameters in this study, we concluded that there was a significant linear relationship between photosynthesis and stomatal conductance in the short term post-HS treatment, but the inhibition of HS on Pn was not the result of stomata closing for longer periods, but rather non-stomata limitation, such as electron transport capacity [57,58]. The increase in G_s and Tr at 4 hpt in HS treated plants may be a self-regulation of plants under stress to decrease leaf surface temperature [59].

Studies have revealed that high temperatures induce anatomical and structural changes in the organization of the photosynthetic membranes of chloroplasts, leading to a decrease in the net photosynthetic rate [60]. In the photosynthesis system, PSII that localized on the thylakoid membrane of chloroplast is often considered as the most heat-sensitive component in the photosynthetic apparatus, whereas PSI has been shown as a heat-resistant component of the photosynthetic electron transport chain [61,62]. In the present study, four genes in PSII were up-regulated at 1 hpt, one gene was up-regulated at 4 hpt, and one gene was up-regulated at R24 hpt. Meanwhile, one and five genes in PSII were down-regulated at 4 hpt and R24 hpt, respectively (Figure 5, Table S3). In PSI, two genes were up-regulated at 1 hpt in HS treated grape leaves, three genes were differentially expressed at 4 hpt. At R24 hpt, 2 and 11 genes in PSI were up-regulated and down-regulated, respectively, indicating PSII was more sensitive to HS than PSI, and high thermal stress may cause serious and perhaps irreversible injury to both PSI and PSII of grapevine leaves [4,62].

As one subunit of the oxygen-evolving complex (OEC) located at the donor side of PSII, the expression of *PsbO* was reduced at R24 hpt, suggesting that HS treatment injures the OEC. Previous studies have proved that *PsbP* and *PsbQ* have specific and important roles in coordinating the activity of the donor and acceptor sides of PSII, and in stabilizing the active form of the PSII-light-harvesting complex II (LHCII) supercomplex [63], *Psb28* was involved in the recovery of PSII at high temperature in *Synechocystis* [64]. In the present study, one *PsbP* gene (*Vitvi04g01013*) and *Psb28* was up-regulated at 1 hpt, and another *PsbP* gene (*Vitvi13g00254*) was up-regulated at 1 and 4 hpt, while the *PsbQ* gene was down-regulated at 4 and R24 hpt (Figure 5, Table S3). From these results, we can assume that genes encoding *PsbP* and *Psb28* play important roles in maintaining or recovery the function of PSII.

High temperature can induce an imbalance between light energy absorption and utilization in photochemical electron transport [65]. Decreases in F_v/F_m are regarded as an indicator of inactivation of PSII reaction centers, caused by damage to the thylakoid membrane [66]. In this study, F_v/F_m was decreased at 1 and 4 hpt in HS-treated grape plants, revealing the electron transfer at the acceptor side of PSII was blocked and the PSII reaction centers was inactivated at 1 and 4 hpt, and was restored its function at R24 hpt. Meanwhile, ABS/CSm was decreased at 1 and 4 hpt, and to a minimum at 4 hpt. ET_o/CSm , TR_o/CSm , and RC/CSm were decreased at all of the three sampling time-points, and to a minimum at 4 hpt, while Dl_o/CSm was increased at 4 and R24 hpt (Figure 4), which suggested that HS treatment impaired the light energy absorption, conversion and electron transfer, as well as decreased the percentage of active reaction centers per cross sections of leaves, and this was another reason for the decreased photosynthetic rate [59,67].

4.2. ABA Biosynthesis, Catabolism and Signal Transduction Was Affected by HS Treatment

High temperature could increase ABA levels in plants by regulating ABA-associated genes and related pathways [20]. Carotenoids are precursors of ABA, and PSY is generally accepted as the most important regulatory enzyme in the biosynthesis of carotenoids and ABA [68]. In this study, two *PSY2* genes (*Vitvi04g02011* and *Vitvi12g00084*) were up-regulated in HS-treated grapevine plants, and the other *PSY2* (*Vitvi06g00084*) was down-regulated at 1 and 4 hpt (Figure 6, Table S4), suggesting the diversity of the expression patterns of *PSYs*. β -carotene hydroxylase (*CrtZ*) could convert β -carotene to zeaxanthin,

and the conversion of zeaxanthin to violaxanthin was affected by the expression level of the gene encoding zeaxanthin epoxidase (ZEP) [69,70]. In HS-treated Kyoho grape leaves, *CrtZ2* (*Vitvi16g01099*) and 1 *ZEP* (*Vitvi04g02205*) were up-regulated at all of the three sampling time-points, 1 *ZEP* (*Vitvi07g01745*) was up-regulated at 1 and 4 hpt in HS-treated grapevine leaves, while *CrtZ1* (*Vitvi02g00020*) was up-regulated at R24 hpt. Two *ZEPs*, *Vitvi06g01061* and *Vitvi02g01811* was up-regulated at 1 and 4 hpt, respectively. *NCED*, which catalyzed the cleavage of 9-*cis*-violaxanthin to produce xanthoxin, has been suggested was the key enzyme in the ABA biosynthetic pathway in plants [71], and the conversion of xanthoxin to abscisic aldehyde catalyzed by *ABA2*, and then to ABA by *AAO3*, were the last steps of the major ABA biosynthetic pathway [72]. In the present study, 3 *NCED* genes and 1 *AAO3* was down-regulated at 1 hpt, but *NCED1* and *NCED4* were up-regulated at 4 and R24 hpt, while *NCED2* was down-regulated at 4 hpt. Another *AAO3* was up-regulated at 1 and 4 hpt in HS-treated grape leaves, and *ABA2* was down-regulated at the three sampling time-points (Figure 6, Table S4).

The ABA catabolism is largely categorized into two types, an irreversible degradation hydroxylated by *ABA8ox* and a reversible conjugation catalyzed by *ABA-GT* [46]. In this study, the expression of *ABA8ox1* was down-regulated at 1 and 4 hpt, *ABA8ox2* was down-regulated at 4 and R24 hpt, while *ABA8ox4* was increased at R24 hpt (Figure 6, Table S4). The expression of *ABA-GT* was decreased at 1 hpt, and increased at R24 hpt, while *CBSX1* was up-regulated at R24 hpt in HS-treated Kyoho leaves (Figure 6, Table S4). These results indicated that less ABA was resolved into PA or transformed into *ABA-GE* at 1 and 4 hpt, while the level of ABA catabolism was enhanced at R24 hpt. Based on these observations, it could be speculated that the ABA level was controlled by the balance between the rates of ABA biosynthesis and catabolism, and regulated by numerous genes involved in the two pathways, as suggested by Nambara and Marion-Poll [21].

ABA signal transduction consists of a double-negative regulatory mechanism, whereby the ABA-bound pyrabactin resistance (PYR)-like (PYL)/regulatory component of ABA receptor (RCAR) inhibit PP2C-type protein phosphatases activity, and PP2C inactivate SnRK2-type protein kinases [73,74]. In the absence of ABA, the receptor forms a homodimer, while the PP2C inhibits autophosphorylation of SnRK2 and phosphorylation of ABF2. In the presence of ABA, a receptor promoter engulfs the hormone within a pocket, allowing the receptor to bind the PP2C and cover the phosphatase active site, thus leads the autophosphorylation of SnRK2 and phosphorylation of its ABF2 substrate. In its phosphorylated form, ABF2 binds to an ABA-responsive element (ABRE) in the promoter of ABA-responsive genes, activating transcription [75]. Additionally, it has been reported that increased ABA content could trigger stomatal closure [76]. Therefore, genes involved in the ABA signaling transduction pathway that induced stomatal closure were identified in this study. Results showed that the ABA content was increased in HS-treated grapevine plants at 1 hpt, the expression of 3 *PYR/PYL*, 4 *PP2C* genes and 1 *ABF* were decreased, while two *SnRK2* were up-regulated at the same time, thus presumably resulting in the stomatal closure. At 4 hpt, the ABA content in HS treated plants was significantly less than that of the control, and the expression of 2 *PYR/PYL*, 2 *PP2C*, 3 *SnRK2*, and 1 *ABF* was down-regulated, while 1 *PP2C*, 2 *SnRK2* and 2 *ABF* were up-regulated, and the *Gs* in HS treated plants was increased. At R24 hpt, lower ABA content was measured in HS-treated plants, 3 *PP2C*, 2 *SnRKs* and 2 *ABF* genes were up-regulated, while 2 *PYR/PYL* and 2 *SnRK2* genes were down-regulated at the same time, possibly contributing to the higher *Gs* in HS-treated plants (Figure 3C, Figure 6 and Figure S3). Thus, there was a positive association between stomatal closure and ABA content in HS treated grapevines.

4.3. Heat Shock Proteins and Heat Shock Factors Were Mostly Up-Regulated by HS Treatment

HSPs play a central role in the response of plants to HS and their acquisition of thermo-tolerance [77]. Previous studies have shown that the heat signal was probably transduced by several pathways to converge on HSFs, followed by activation of a number of HSPs and other heat-responsive genes that drive the heat adaptation process in plants [78–80]. HSP

families include HSP100 (Clp), HSP90, HSP70 (DnaK), HSP60 (chaperonin and GroEL) and small HSPs (sHSPs) [81]. Sixty-eight DEGs were identified in our study as candidate genes for membership in different HSP families. Most of the HSPs were significantly up-regulated during the heat treatment and the following recovery, and the expression level of some was sharply increased at 1 hpt and reduced gradually (Figure 7A, Table S5), which was consistent with previous study that plants suffering from HS sharply accumulated HSPs to enhance heat tolerance [82]. It has been confirmed that sHSPs played an important role in heat tolerance [83,84]. Wheat chloroplastic *sHSP26* was highly induced by HS in vegetative and generative tissues in both wheat and *Arabidopsis* [85]. In the present study, differentially expressed sHSPs accounted for the total differentially expressed HSPs 66.18%, evidencing their importance (Figure 7A, Table S5).

HSFs play important roles in both basal and acquired thermotolerance through binding to *cis*-acting regulatory elements called heat shock elements (HSEs) in the promoter region of HSP genes [80]. Four *HSEA3* homologous genes were identified in transcriptome of HS treated Rhododendron, and their expression levels were increased by 10,000-fold after heat treatment for 24 h [86]. In our study, one *HSEA3* was identified, and it was up-regulated at 4 and R24 hpt, suggesting this gene could not sense the HS immediately (Figure 7B, Table S6). In grapevine, both *VvHSEA2a* and *VpHSFB2b* have been reported to be associated with thermotolerance [27,28]. In this study, *HSFB2b* was also up-regulated in HS-treated Kyoho leaves in all of the three sampling time-points, but no *HSEA2a* was identified (Figure 7). It should be noted that the expression levels of 2 HSFs were decreased post-HS treatment (Figure 7B, Table S6), thus, it could be speculated that these genes functioned negatively in the heat tolerance of grapevine.

It should be noted that most HSFs and HSPs maintained similar heat response profiles among subgenomes, indicating little functional divergence occurred among the orthologous genes of HSFs and HSPs, as suggested by Wang et al. [87].

5. Conclusions

The study provided evidence to suggest that PSII was more sensitive to HS than PSI, and genes encoding *PsbP* and *Psb28* played important roles in maintaining the function of PSII. HS treatment impaired the photosynthetic capacity of grapevine leaves, and there was a significant positive relationship between photosynthesis and stomatal conductance in the short term post-HS treatment, but the inhibition of HS on *Pn* was non-stomata limitation for a longer period. The ABA content in HS-treated Kyoho plants was higher than that in the control at 1 hpt, but less in HS-treated plants at 4 and R24 hpt, which was regulated by numerous genes involved in the ABA biosynthesis and catabolism pathways. Most differentially expressed *HSFs* and *HSPs* encoding sequences, especially *HSF30*, *HSEA6b*, *HSFB2a*, *HSFB2b* and *sHSPs*, played important roles in response to HS treatment. These results provide candidate genes and pathways involved in the HS responses in grapevine, especially deepening our understanding of relationship between photosynthesis, ABA biosynthesis, metabolism, signal transduction and HS in grapevine.

Supplementary Materials: The following supporting information can be downloaded at: at <https://www.mdpi.com/article/10.3390/agronomy12102591/s1>, Figure S1: Principal component analysis of RNA-seq data (A) and correlation of transcriptome profiles among samples post-HS treatment and control (B). Figure S2: Validation of the gene expression results of qRT-PCR and RNA-seq in the HS-treated grapevines and control. Figure S3: ABA content in HS-treated grapevines and control at 1, 4 and R24 hpt. Data represent mean values \pm SD from three independent experiments. Asterisks indicate statistical significance (* $0.01 < p < 0.05$, ** $p < 0.01$, Student's *t*-test) of differences between HS-treated grapevines and control. Table S1. List of the primers used for quantitative real-time RT-PCR validation experiments. Table S2. Summary of Illumina reads mapping to the reference grapevine genome by BLAST analysis. Table S3. Transcriptomic profiles and annotation of DEGs involved in photosynthesis pathway following HS treatment and subsequent recovery. Table S4. Transcriptomic profiles and annotation of DEGs involved in the ABA biosynthesis, metabolism, and signal transduction pathways following HS treatment and subsequent recovery. Table S5.

Transcriptomic profiles and annotation of DEGs contained in HSP family following HS treatment and subsequent recovery. Table S6. Transcriptomic profiles and annotation of DEGs contained in HSF family following HS treatment and subsequent recovery.

Author Contributions: Conceptualization, R.G. and X.C.; methodology, L.L., G.H. and S.Z.; software, R.W. and X.S.; investigation, J.H. and Y.Z.; writing, R.G. and X.C.; supervision, T.X. and X.B.; funding acquisition, R.G. and X.C. All authors have read and agree to the published version of the manuscript.

Funding: This research was funded by the National Natural Science Foundation of China (31860543 and 31760554), as well as the Science and Technology Development Fund of Guangxi Academy of Agricultural Sciences (Guinongke Grant No. 31860543, Guinongke2021JM26 and 2018JZ22).

Data Availability Statement: The RNA-seq rawdata has been deposited in the NCBI Sequence Read Archive under the accession number PRJNA752263 (<https://www.ncbi.nlm.nih.gov/bioproject/PRJNA752263>, accessed on 5 August 2021).

Acknowledgments: We thank Biomarker Technologies for their help with high-throughput-sequencing-related experiments.

Conflicts of Interest: The authors declare that they have no known competing financial interests or personal relationships that could have appeared to influence the work reported in this paper.

Abbreviations

HS	heat stress
ABA	abscisic acid
HSFs	heat shock transcription factors
HSPs	heat shock proteins
iiTRAQ	isobaric tags for relative and absolute quantitation
qRT-PCR	quantitative real-time RT-PCR
FPKM	fragments per kilobase of transcript per million mapped reads
NR	NCBI non-redundant protein sequence database
COG	Cluster of Orthologous Groups
Pfam	The database of Homologous protein family
KEGG	The database of Kyoto Encyclopedia of Genes and Genomes
GO	Gene Ontology
DEGs	differentially expressed genes
Pn	Net photosynthetic rate
Gs	stomatal conductance
Ci	substomatal CO ₂ concentration
Tr	transpiration rate
PPFD	photosynthetic photon flux density
PSII	photosystem II
PSI	photosystem I
Fv/Fm	maximum quantum efficiency of PSII photochemistry
C _{Sm}	excited leaf cross-section
ABS/C _{Sm}	absorption flux per C _{Sm} approximated
TRo/C _{Sm}	trapped energy flux per C _{Sm}
RC/C _{Sm}	percentage of active/inactive reaction centers per C _{Sm}
ETo/C _{Sm}	electron transport flux per C _{Sm}
DIo/C _{Sm}	dissipated energy flux per C _{Sm}
Hpt	hour post treatment
R24 hpt	24 h after recovery from treatment
PSY	phytoene synthase
CrtZ	beta-carotene hydroxylase
ZEP	zeaxanthin epoxidase
NCED	9-cis-epoxycarotenoid dioxygenase
ABAO	abscisic-aldehyde oxidase
ABA8ox	ABA 8'-hydroxylase
ABA-GT	ABA glucosyltransferase

PA	phaseic acid
ABA-GE	ABA glucosyl-ester
PP2C	type 2C serine threonine protein phosphatase
SnRK2	SNF1-related type 2 protein kinases
ABF	ABA-responsive element binding factor
ABI	ABA-insensitive
OEC	oxygen-evolving complex
LHCII	PSII-light-harvesting complex II

References

- Vivier, M.A.; Pretorius, I.S. Genetically tailored grapevines for the wine industry. *Trends Biotechnol.* **2002**, *20*, 472–478. [[CrossRef](#)]
- Cramer, G.; Urano, K.; Delrot, S.; Pezzotti, M.; Shinozaki, K. Effects of abiotic stress on plants: A systems biology perspective. *BMC Plant Biol.* **2011**, *11*, 163. [[CrossRef](#)] [[PubMed](#)]
- Xu, H.G.; Liu, G.J.; Liu, G.T.; Yan, B.F.; Duan, W.; Wang, L.J.; Li, S.H. Comparison of investigation methods of heat injury in grapevine (*Vitis*) and assessment to heat tolerance in different cultivars and species. *BMC Plant Biol.* **2014**, *14*, 156. [[CrossRef](#)] [[PubMed](#)]
- Venios, X.; Korkas, E.; Nisiotou, A.; Banilas, G. Grapevine responses to heat stress and global warming. *Plants* **2020**, *9*, 1754. [[CrossRef](#)] [[PubMed](#)]
- Liu, G.T.; Wang, J.F.; Cramer, G.; Dai, Z.W.; Duan, W.; Xu, H.G.; Wu, B.H.; Fan, P.G.; Wang, L.J.; Li, S.H. Transcriptomic analysis of grape (*Vitis vinifera* L.) leaves during and after recovery from heat stress. *BMC Plant Biol.* **2012**, *12*, 174. [[CrossRef](#)] [[PubMed](#)]
- Cohen, S.D.; Tarara, J.M.; Gambetta, G.A.; Matthews, M.A.; Kennedy, J.A. Impact of diurnal temperature variation on grape berry development, proanthocyanidin accumulation, and the expression of flavonoid pathway genes. *J. Exp. Bot.* **2012**, *63*, 2655–2665. [[CrossRef](#)]
- Greer, D.H.; Weedon, M.M. The impact of high temperatures on *Vitis vinifera* cv. Semillon grapevine performance and berry ripening. *Front. Plant Sci.* **2013**, *4*, 491. [[CrossRef](#)]
- Zhang, J.H.; Huang, W.D.; Liu, Y.P.; Pan, Q.H. Effects of temperature acclimation pretreatment on the ultrastructure of mesophyll cells in young grape plants (*Vitis vinifera* L. cv. Jingxiu) under cross-temperature stresses. *J. Integr. Plant Biol.* **2005**, *47*, 959–970. [[CrossRef](#)]
- Kriedemann, P.E. Photosynthesis in vine leaves as a function of light intensity, temperature and leaf age. *Vitis* **1968**, *7*, 213–220.
- Ferrini, F.; Mattii, G.B.; Nicese, F.P. Effect of temperature on key physiological responses of grapevine leaf. *Am. J. Enol. Viticult.* **1995**, *46*, 375–379.
- Schultz, H.R. Extension of a Farquhar model for limitations of leaf photosynthesis induced by light environment, phenology and leaf age in grapevines (*Vitis vinifera* L. cv. White Riesling and Zinfandel). *Funct. Plant Biol.* **2003**, *30*, 673–687. [[CrossRef](#)]
- Yu, D.J.; Kim, S.J.; Lee, H.J. Stomatal and non-stomatal limitations to photosynthesis in field-grown grapevine cultivars. *Biol. Plant.* **2009**, *53*, 133–137. [[CrossRef](#)]
- Zsofi, Z.; Varadi, G.; Balo, B.; Marschall, M.; Nagy, Z. Heat acclimation of grapevine leaf photosynthesis: Mezzo- and macroclimate aspects. *Funct. Plant Biol.* **2009**, *36*, 310–322. [[CrossRef](#)]
- Luo, H.B.; Ma, L.; Xi, H.F.; Duan, W.; Li, S.H.; Loescher, W.; Wang, J.F.; Wang, L.J. Photosynthetic responses to heat treatments at different temperatures and following recovery in grapevine (*Vitis amurensis* L.) leaves. *PLoS ONE* **2011**, *6*, e23033. [[CrossRef](#)]
- Wang, L.J.; Fan, L.; Loescher, W.; Duan, W.; Liu, G.J.; Cheng, J.S.; Luo, H.B.; Li, S.H. Salicylic acid alleviates decreases in photosynthesis under heat stress and accelerates recovery in grapevine leaves. *BMC Plant Biol.* **2010**, *10*, 34. [[CrossRef](#)]
- Greer, D.H.; Weedon, M.M. Modelling photosynthetic responses to temperature of grapevine (*Vitis vinifera* cv. Semillon) leaves on vines grown in a hot climate. *Plant Cell Environ.* **2012**, *35*, 1050–1064. [[CrossRef](#)]
- Greer, D.H.; Weston, C. Heat stress affects flowering, berry growth, sugar accumulation and photosynthesis of *Vitis vinifera* cv. Semillon grapevines grown in a controlled environment. *Funct. Plant Biol.* **2010**, *37*, 206–214. [[CrossRef](#)]
- Sepulveda, G.; Kliewer, W.M. Stomatal response of three grapevine cultivars (*Vitis vinifera* L.) to high temperature. *Am. J. Enol. Vitic.* **1986**, *37*, 44–52.
- Baron, K.N.; Schroeder, D.F.; Stasolla, C. Transcriptional response of abscisic acid (ABA) metabolism and transport to cold and heat stress applied at the reproductive stage of development in *Arabidopsis thaliana*. *Plant Sci.* **2012**, *188–189*, 48–59. [[CrossRef](#)]
- Sharma, E.; Borah, P.; Kaur, A.; Bhatnagar, A.; Mohapatra, T.; Kapoor, S.; Khurana, J.P. A comprehensive transcriptome analysis of contrasting rice cultivars highlights the role of auxin and ABA responsive genes in heat stress response. *Genomics* **2021**, *113*, 1247–1261. [[CrossRef](#)]
- Nambara, E.; Marion-Poll, A. Abscisic acid biosynthesis and catabolism. *Annu. Rev. Plant Biol.* **2005**, *56*, 165–185. [[CrossRef](#)]
- Larkindale, J.; Hall, J.D.; Knight, M.R.; Vierling, E. Heat stress phenotypes of *Arabidopsis* mutants implicate multiple signaling pathways in the acquisition of thermotolerance. *Plant Physiol.* **2005**, *138*, 882–897. [[CrossRef](#)]
- Larkindale, J.; Huang, B. Thermotolerance and antioxidant systems in *Agrostis stolonifera*: Involvement of salicylic acid, abscisic acid, calcium, hydrogen peroxide, and ethylene. *J. Plant Physiol.* **2004**, *161*, 405–413. [[CrossRef](#)]
- Gong, M.; Li, Y.J.; Chen, S.Z. Abscisic acid induced thermotolerance in maize seedlings is mediated by Ca²⁺ and associated with antioxidant systems. *J. Plant Physiol.* **1998**, *153*, 615–621. [[CrossRef](#)]

25. Robertson, A.J.; Ishikawa, M.; Gusta, L.V.; MacKenzie, S.L. Abscisic acid-Induced heat tolerance in bromus inermis leys cell-suspension cultures (heat-stable, abscisic acid-responsive polypeptides in combination with sucrose confer enhanced thermostability). *Plant Physiol.* **1994**, *105*, 181–190. [[CrossRef](#)]
26. Zarrouk, O.; Brunetti, C.; Egipto, R.; Pinheiro, C.; Genebra, T.; Gori, A.; Lopes, C.M.; Tattini, M.; Chaves, M.M. Grape ripening is regulated by deficit irrigation/elevated temperatures according to cluster position in the canopy. *Front. Plant Sci.* **2016**, *7*, 1640. [[CrossRef](#)]
27. Pillet, J.; Egert, A.; Pieri, P.; Lecourieux, F.; Kappel, C.; Charon, J.; Gomes, E.; Keller, F.; Delrot, S.; Lecourieux, D. *VvGOLS1* and *VvHsfA2* are involved in the heat stress responses in grapevine berries. *Plant Cell Physiol.* **2012**, *53*, 1776–1792. [[CrossRef](#)]
28. Peng, S.B.; Zhu, Z.G.; Zhao, K.; Shi, J.L.; Yang, Y.Z.; He, M.Y.; Wang, Y.J. A novel heat shock transcription factor, *VpHsf1*, from Chinese Wild *Vitis pseudoreticulata* is involved in biotic and abiotic stresses. *Plant Mol. Biol. Rep.* **2013**, *31*, 240–247. [[CrossRef](#)]
29. Liu, G.T.; Chai, F.M.; Wang, Y.; Jiang, J.Z.; Duan, W.; Wang, Y.T.; Wang, F.F.; Li, S.H.; Wang, L.J. Genome-wide identification and classification of HSF family in grape, and their transcriptional analysis under heat acclimation and heat stress. *Hortic. Plant J.* **2018**, *4*, 133–143. [[CrossRef](#)]
30. Kobayashi, M.; Katoh, H.; Takayanagi, T.; Suzuki, S. Characterization of thermotolerance-related genes in grapevine (*Vitis vinifera*). *J. Plant Physiol.* **2010**, *167*, 812–819. [[CrossRef](#)]
31. Kobayashi, M.; Takato, H.; Fujita, K.; Suzuki, S. *HSG1*, a grape Bcl-2-associated athanogene, promotes floral transition by activating CONSTANS expression in transgenic *Arabidopsis* plant. *Mol. Biol. Rep.* **2012**, *39*, 4367–4374. [[CrossRef](#)] [[PubMed](#)]
32. Liu, G.T.; Ma, L.; Duan, W.; Wang, B.C.; Li, J.H.; Xu, H.G.; Yan, X.Q.; Yan, B.F.; Li, S.H.; Wang, L.J. Differential proteomic analysis of grapevine leaves by iTRAQ reveals responses to heat stress and subsequent recovery. *BMC Plant Biol.* **2014**, *14*, 110. [[CrossRef](#)] [[PubMed](#)]
33. Jiang, J.F.; Liu, X.N.; Liu, C.H.; Liu, G.T.; Li, S.H.; Wang, L.J. Integrating omics and alternative splicing reveals insights into grape response to high temperature. *Plant Physiol.* **2017**, *173*, 1502–1518. [[CrossRef](#)] [[PubMed](#)]
34. Rienth, M.; Torregrosa, L.; Sarah, G.; Ardisson, M.; Brillouet, J.-M.; Romieu, C. Temperature desynchronizes sugar and organic acid metabolism in ripening grapevine fruits and remodels their transcriptome. *BMC Plant Biol.* **2016**, *16*, 164. [[CrossRef](#)]
35. Pucker, B.; Schwandner, A.; Becker, S.; Hausmann, L.; Viehöver, P.; Töpfer, R.; Weisshaar, B.; Holtgräwe, D. RNA-Seq time series of *Vitis vinifera* bud development reveals correlation of expression patterns with the local temperature profile. *Plants* **2020**, *9*, 1548. [[CrossRef](#)]
36. Touns, H.S.; Cochetel, N.; Gray, D.; Cramer, G.R. *VviERF6Ls*: An expanded clade in *Vitis* responds transcriptionally to abiotic and biotic stresses and berry development. *BMC Genom.* **2020**, *21*, 472. [[CrossRef](#)]
37. Jallion, O.; Aury, J.M.; Noel, B.; Policriti, A.; Clepet, C.; Casagrande, A.; Choisne, N.; Aubourg, S.; Vitulo, N.; Jubin, C.; et al. The grapevine genome sequence suggests ancestral hexaploidization in major angiosperm phyla. *Nature* **2007**, *449*, 463–467.
38. Kim, D.; Langmead, B.; Salzberg, S.L. HISAT: A fast spliced aligner with low memory requirements. *Nat. Methods* **2015**, *12*, 357–360. [[CrossRef](#)]
39. Trapnell, C.; Williams, B.A.; Pertea, G.; Mortazavi, A.; Kwan, G.; van Baren, M.J.; Salzberg, S.L.; Wold, B.J.; Pachter, L. Transcript assembly and quantification by RNA-Seq reveals unannotated transcripts and isoform switching during cell differentiation. *Nat. Biotechnol.* **2010**, *28*, 511–515. [[CrossRef](#)]
40. Love, M.I.; Huber, W.; Anders, S. Moderated estimation of fold change and dispersion for RNA-seq data with DESeq2. *Genome Biol.* **2014**, *15*, 550. [[CrossRef](#)]
41. Young, M.D.; Wakefield, M.J.; Smyth, G.K.; Oshlack, A. Gene ontology analysis for RNA-seq: Accounting for selection bias. *Genome Biol.* **2010**, *11*, R14. [[CrossRef](#)]
42. Mao, X.; Cai, T.; Olyarchuk, J.G.; Wei, L. Automated genome annotation and pathway identification using the KEGG Orthology (KO) as a controlled vocabulary. *Bioinformatics* **2005**, *21*, 3787–3793. [[CrossRef](#)]
43. Livak, K.J.; Schmittgen, T.D. Analysis of relative gene expression data using real-time quantitative PCR and the $2^{-\Delta\Delta CT}$ method. *Methods* **2001**, *25*, 402–408. [[CrossRef](#)]
44. Sitko, K.; Rusinowski, S.; Pogrzeba, M.; Daszkowska-Golec, A.; Gieroń, Ż.; Kalaji, H.; Małkowski, E. Development and aging of photosynthetic apparatus of *Vitis vinifera* L. during growing season. *Photosynthetica* **2020**, *58*, 186–193. [[CrossRef](#)]
45. Yang, J.C.; Zhang, J.H.; Wang, Z.Q.; Zhu, Q.S.; Wang, W. Hormonal changes in the grains of rice subjected to water stress during grain filling. *Plant J.* **2001**, *127*, 315–323. [[CrossRef](#)]
46. Chen, W.K.; Yu, K.J.; Liu, B.; Lan, Y.B.; Sun, R.Z.; Li, Q.; He, F.; Pan, Q.H.; Duan, C.Q.; Wang, J. Comparison of transcriptional expression patterns of carotenoid metabolism in ‘Cabernet Sauvignon’ grapes from two regions with distinct climate. *J. Plant Physiol.* **2017**, *213*, 75–86. [[CrossRef](#)]
47. Ohama, N.; Sato, H.; Shinozaki, K.; Yamaguchi-Shinozaki, K. Transcriptional regulatory network of plant heat stress response. *Trends Plant Sci.* **2017**, *22*, 53–65. [[CrossRef](#)]
48. Ju, Y.; Min, Z.; Zhang, Y.; Zhang, K.-k.; Liu, M.; Fang, Y. Transcriptome profiling provide new insights into the molecular mechanism of grapevine response to heat, drought, and combined stress. *Sci. Hortic.* **2021**, *286*, 110076. [[CrossRef](#)]
49. Liu, M.; Ju, Y.; Min, Z.; Fang, Y.; Meng, J. Transcriptome analysis of grape leaves reveals insights into response to heat acclimation. *Sci. Hortic.* **2020**, *272*, 109554. [[CrossRef](#)]
50. Coate, J.E.; Doyle, J.J. Quantifying whole transcriptome size, a prerequisite for understanding transcriptome evolution across species: An example from a plant allopolyploid. *Genome Biol. Evol.* **2010**, *2*, 534–546. [[CrossRef](#)]

51. Pirrello, J.; Deluche, C.; Frangne, N.; Gévaudant, F.; Maza, E.; Djari, A.; Bourge, M.; Renaudin, J.-P.; Brown, S.; Bowler, C.; et al. Transcriptome profiling of sorted endoreduplicated nuclei from tomato fruits: How the global shift in expression ascribed to DNA ploidy influences RNA-Seq data normalization and interpretation. *Plant J.* **2018**, *93*, 387–398. [[CrossRef](#)]
52. Sharma, A.; Kumar, V.; Shahzad, B.; Ramakrishnan, M.; Singh Sidhu, G.P.; Bali, A.S.; Handa, N.; Kapoor, D.; Yadav, P.; Khanna, K.; et al. Photosynthetic response of plants under different abiotic stresses: A Review. *J. Plant Growth Regul.* **2020**, *39*, 509–531. [[CrossRef](#)]
53. Li, Y.T.; Xu, W.W.; Ren, B.Z.; Zhao, B.; Zhang, J.W.; Liu, P.; Zhang, Z.S. High temperature reduces photosynthesis in maize leaves by damaging chloroplast ultrastructure and photosystem II. *J. Agron. Crop Sci.* **2020**, *00*, 1–17. [[CrossRef](#)]
54. Allario, T.; Brumos, J.; Colmenero-Flores, J.M.; Iglesias, D.J.; Pina, J.A.; Navarro, L.; Talon, M.; Ollitrault, P.; Morillon, R. Tetraploid Rangpur lime rootstock increases drought tolerance via enhanced constitutive root abscisic acid production. *Plant Cell Environ.* **2013**, *36*, 856–868. [[CrossRef](#)]
55. Matsui, A.; Ryugo, K.; Kliewer, W.M. Lowered berry quality due to heat stress at the early ripening stage of berry growth in a seeded grapevine, *Vitis vinifera* L. *Res. Bull. Fac. Agric. Gifu Univ.* **1991**, *56*, 139–145.
56. Godde, D.; Bormann, J.F. Regulation of photosynthesis in higher plants. In *Molecular to Global Photosynthesis*; Archer, M.D., Barber, J., Eds.; Imperial College Press: London, UK, 2004; pp. 221–286.
57. Salvucci, M.E.; Crafts-Brandner, S.J. Relationship between the heat tolerance of photosynthesis and the thermal stability of rubisco activase in plants from contrasting thermal environments. *Plant Physiol.* **2004**, *134*, 1460–1470. [[CrossRef](#)]
58. Way, D.A.; Oren, R. Differential responses to changes in growth temperature between trees from different functional groups and biomes: A review and synthesis of data. *Physiology* **2010**, *30*, 669–688. [[CrossRef](#)]
59. Feng, B.; Liu, P.; Li, G.; Dong, S.T.; Wang, F.H.; Kong, L.A.; Zhang, J.W. Effect of Heat Stress on the Photosynthetic characteristics in flag leaves at the grain-filling stage of different heat-resistant winter wheat varieties. *J. Agron. Crop Sci.* **2014**, *200*, 143–155. [[CrossRef](#)]
60. Bernardo, S.; Dinis, L.-T.; Machado, N.; Moutinho-Pereira, J. Grapevine abiotic stress assessment and search for sustainable adaptation strategies in Mediterranean-like climates. A review. *Agron. Sustain. Dev.* **2018**, *38*, 66. [[CrossRef](#)]
61. Brestic, M.; Zivcak, M.; Olsovska, K.; Kalaji, H.M.; Shao, H.B.; Hakeem, K.R. Heat signaling and stress responses in photosynthesis. In *Plant Signaling: Understanding the Molecular Crosstalk*; Hakeem, K.R., Rehman, R.U., Tahir, I., Eds.; Springer: New Delhi, India, 2014; pp. 241–256.
62. Kun, Z.; Bai-hong, C.; Yan, H.; Rui, Y.; Yu-an, W. Effects of short-term heat stress on PSII and subsequent recovery for senescent leaves of *Vitis vinifera* L. cv. Red Globe. *J. Integr. Agr.* **2018**, *17*, 2683–2693.
63. Ifuku, K.; Ido, K.; Sato, F. Molecular functions of PsbP and PsbQ proteins in the photosystem II supercomplex. *J. Photochem. Photobiol. B Biol.* **2011**, *104*, 158–164. [[CrossRef](#)] [[PubMed](#)]
64. Sakata, S.; Mizusawa, N.; Kubota-Kawai, H.; Sakurai, I.; Wada, H. Psb28 is involved in recovery of photosystem II at high temperature in *Synechocystis* sp. PCC 6803. *B.B.A. Bioenerg.* **2013**, *1827*, 50–59. [[CrossRef](#)] [[PubMed](#)]
65. Wang, L.J.; Loescher, W.; Duan, W.; Li, W.D.; Yang, S.H.; Li, S.H. Heat acclimation induced acquired heat tolerance and cross adaptation in different grape cultivars: Relationships to photosynthetic energy partitioning. *Funct. Plant Biol.* **2009**, *36*, 516–526. [[CrossRef](#)] [[PubMed](#)]
66. Roháček, K. Chlorophyll fluorescence parameters: The definitions, photosynthetic meaning, and mutual relationships. *Photosynthetica* **2002**, *40*, 13–29. [[CrossRef](#)]
67. Zhang, Q.C.; Li, Y.; Xu, W.G.; Zhang, Y.; Qi, X.L.; Fang, Y.H.; Peng, C.J. Joint expression of *Zmpepc*, *Zmppdk*, and *Zmnadp-me* is more efficient than expression of one or two of those genes in improving the photosynthesis of *Arabidopsis*. *Plant Physiol. Biochem.* **2021**, *158*, 410–419. [[CrossRef](#)]
68. Cazzonelli, C.I.; Pogson, B.J. Source to sink: Regulation of carotenoid biosynthesis in plants. *Trends Plant Sci.* **2010**, *5*, 266–274. [[CrossRef](#)]
69. Guzman, I.; Hamby, S.; Romero, J.; Bosland, P.W.; O’Connell, M.A. Variability of carotenoid biosynthesis in orange colored *Capsicum* spp. *Plant Sci.* **2010**, *179*, 49–59. [[CrossRef](#)]
70. Sugiyama, A.; Ikoma, Y.; Fujii, H.; Shimada, T.; Endo, T.; Shimizu, T.; Omura, M. Structure and expression levels of alleles of *Citrus* zeaxanthin epoxidase genes. *J. Jpn. Soc. Hort. Sci.* **2010**, *79*, 263–274. [[CrossRef](#)]
71. Zhang, M.; Leng, P.; Zhang, G.L.; Li, X.X. Cloning and functional analysis of 9-*cis*-epoxycarotenoid dioxygenase (NCED) genes encoding a key enzyme during abscisic acid biosynthesis from peach and grape fruits. *J. Plant Physiol.* **2009**, *166*, 1241–1252. [[CrossRef](#)]
72. Seo, M.; Koshiba, T. Complex regulation of ABA biosynthesis in plants. *Trends Plant Sci.* **2002**, *7*, 41–48. [[CrossRef](#)]
73. Boneh, U.; Biton, I.; Schwartz, A.; Ben-Ari, G. Characterization of the ABA signal transduction pathway in *Vitis vinifera*. *Plant Sci.* **2012**, *187*, 89–96. [[CrossRef](#)]
74. Lee, S.C.; Luan, S. ABA signal transduction at the crossroad of biotic and abiotic stress responses. *Plant Cell Environ.* **2012**, *35*, 53–60. [[CrossRef](#)]
75. Klingler, J.P.; Batelli, G.; Zhu, J.K. ABA receptors: The START of a new paradigm in phytohormone signalling. *J. Exp. Bot.* **2010**, *61*, 3199–3210. [[CrossRef](#)]
76. Schroeder, J.I.; Allen, G.J.; Hugouvieux, V.; Kwak, J.M.; Waner, D. Guard cell signal transduction. *Annu. Rev. Plant Physiol. Plant Biol.* **2001**, *52*, 627–658. [[CrossRef](#)]

77. Sun, J.; Ren, L.P.; Cheng, Y.; Gao, J.J.; Dong, B.; Chen, S.M.; Chen, F.D.; Jiang, J.F. Identification of differentially expressed genes in *Chrysanthemum nankingense* (Asteraceae) under heat stress by RNA Seq. *Gene* **2014**, *552*, 59–66. [[CrossRef](#)]
78. Bokszczanin, K.L.; Fragkostefanakis, S. Perspectives on deciphering mechanisms underlying plant heat stress response and thermotolerance. *Front. Plant Sci.* **2013**, *4*, 315. [[CrossRef](#)]
79. Kotak, S.; Larkindale, J.; Lee, U.; Koskull-Doring, P.V.; Vierling, E.; Scharf, K.D. Complexity of the heat stress response in plants. *Curr. Opin. Plant Biol.* **2007**, *10*, 310–316. [[CrossRef](#)]
80. Saidi, Y.; Finka, A.; Goloubinoff, P. Heat perception and signalling in plants: A tortuous path to thermotolerance. *New Phytol.* **2011**, *190*, 556–565. [[CrossRef](#)]
81. Huang, B.R.; Xu, C.P. Identification and characterization of proteins associated with plant tolerance to heat stress. *J. Integr. Plant Biol.* **2008**, *50*, 1230–1237. [[CrossRef](#)]
82. Wahid, A.; Gelani, S.; Ashraf, M.; Foolad, M.R. Heat tolerance in plants: An overview. *Environ. Exp. Bot.* **2007**, *61*, 199–223. [[CrossRef](#)]
83. Heckathorn, S.A.; Downs, C.A.; Sharker, T.D.; Coleman, J.S. The small, methionine-rich chloroplast heat-shock protein protects photosystem II electron transport during heat stress. *Plant Physiol.* **1998**, *116*, 439–444. [[CrossRef](#)]
84. Sanmiya, K.; Suzuki, K.; Egawa, Y.; Shono, M. Mitochondrial small heat-shock protein enhances thermotolerance in tobacco plants. *FEBS Lett.* **2004**, *557*, 265–268. [[CrossRef](#)]
85. Chuang, H.; Khurana, N.; Nijhavan, A.; Khurana, J.P.; Khurana, P. The wheat chloroplastic small heat shock protein (sHSP26) is involved in seed maturation and germination and imparts tolerance to heat stress. *Plant Cell Environ.* **2012**, *35*, 1912–1931.
86. Fang, L.C.; Tong, J.; Dong, Y.F.; Xu, D.Y.; Mao, J.; Zhou, Y. De novo RNA sequencing transcriptome of *Rhododendron obtusum* identified the early heat response genes involved in the transcriptional regulation of photosynthesis. *PLoS ONE* **2017**, *12*, e0186376. [[CrossRef](#)]
87. Wang, X.M.; Chen, S.Y.; Shi, X.; Liu, D.N.; Zhao, P.; Lu, Y.Z.; Cheng, Y.B.; Liu, Z.S.; Nie, X.J.; Song, W.N.; et al. Hybrid sequencing reveals insight into heat sensing and signaling of bread wheat. *Plant J.* **2019**, *98*, 1015–1032. [[CrossRef](#)]